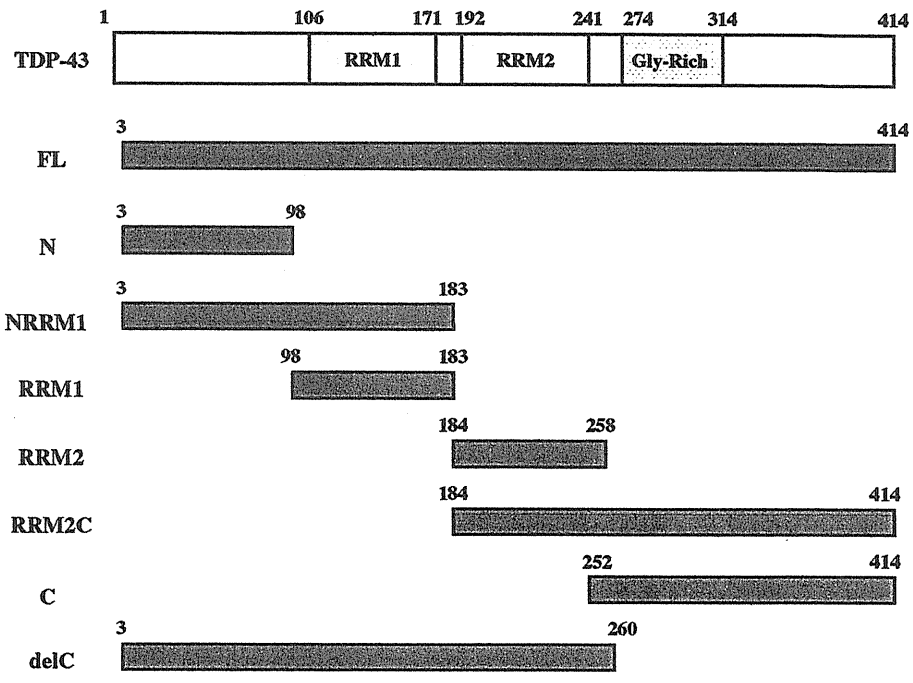

Fig. 1 The structural domains of the human TDP-43 protein. The domain structure of the human TDP-43 protein is shown on the *top* with the position of amino acid residues. The genes encoding the full-length (*FL*) TDP-43 protein and a panel of truncated forms, such as the C-terminal domain-cleaved protein (*delC*), the C-terminal domain fragment (*C*), the N-terminal domain fragment (*N*), *RRM1*, *RRM2*, the N-terminal domain plus RRM1 (*NRRM1*), and the C-terminal domain plus RRM2 (*RRM2C*), were cloned in the expression vectors as listed in Table 1

of TDP-43 were cloned in the vector pFN21A-CMV Flexi (Table 1), and transfected in HEK293 cells. 24 h after transfection, the live cells were exposed for 15 min to Oregon Green (Promega), a fluorochrome specifically bound to the Halo tag protein, fixed in 4% paraformaldehyde, and exposed to 4′,6′-diamidino-2-phenylindole (DAPI). They were mounted with glycerol-polyvinyl alcohol and examined under the Olympus BX51 universal microscope.

Results

Constitutive Expression of TDP-43 Dimer in Human Cell Cultures

By Western blot of the detergent-soluble protein extract with anti-TDP-43 antibody (10782-2-AP), HEK293, HeLa, and SK-N-SH cells in culture expressed constitutively a major 43-kDa protein representing the full-length (FL) TDP-43 protein, variable levels of 36- and 27-kDa proteins representing the N-terminally cleaved fragments, and a small but discernible amount of the 86-kDa protein (Fig. 2, panels a–c, lane 1). By densitometric analysis, the 86-kDa protein consisted of approximately 4% of total TDP-43-immunoreactive proteins in HEK293 cells, where minimum 50 μg of protein is required for loading on the gel to detect the 86-kDa protein. A 24-h treatment of the cells with MG-132, an inhibitor of proteasome function, did not alter the expression levels of the 86-kDa protein (Fig. 2, panels a–c, lane 2).

Because the 86-kDa TDP-43-immunoreactive protein has not been reported previously, we assumed that it represents a fairly small fraction of the endogenous FL TDP-43 dimer, based on its molecular weight. First, to characterize this protein, we concentrated both 86- and 43-kDa proteins extracted from the corresponding SDS–PAGE gel bands. They were then processed for Western blot analysis using anti-TDP-43 antibody (10782-2-AP) that reacts with amino acid residues 1–260 located at the N-terminal half or anti-TDP-43 antibody (NB110-55376) that reacts with amino acid residues 350–414 located at the C-terminus of the human TDP-43 protein. Both antibodies recognized the 86-kDa protein, along with the 43-kDa protein (Fig. 3A, panels a and b, lanes 1 and 2). In contrast, the exclusion of the primary antibodies did not react with either (Fig. 3A, panel c, lanes 1 and 2). These results argue against the possibility that the 86-kDa protein reflects a protein of non-TDP43 origin that simply exhibits cross-reactivity to TDP-43 on the blot. Furthermore, transient expression of the siRNA vector targeted specifically to TDP-43 but not to a scrambled sequence substantially reduced the expression of both 43- and 86-kDa TDP-43 immunoreactive proteins, suggesting that the 86-kDa protein is composed of TDP-43 (Fig. 3B, panels a and b, lanes 2 and 3).

Overexpression of ubiqulin-1 (UBQLN1), a proteasome-targeting factor that promotes the formation of cytoplasmic aggregations of TDP-43 (Kim et al. 2008) or casein kinase-1 alpha-1 (CSNK1A1), a protein kinase that mediates phosphorylation of major serine epitopes in the C-terminal domain of TDP-43 (Kametani et al. 2009), did not change the levels of expression of the 86-kDa protein in HEK293

Table 1 Primers utilized for PCR-based cloning in this study

Genes	Cloning vectors	Restriction enzyme sites for cloning	Sense primers	Antisense primers
TDP-43 (the full-length: amino acid residues 3-414; FL)	p3XFLAG-CMV7.1	KpnI, XbaI	5′ggggtacccctgtctgaatatattcgggta3′	5′gctctagagcctacattccccagccagaag3′
TDP-43 (deletion of the C-terminus: amino acid residues 3-260; delC)	p3XFLAG-CMV7.1	KpnI, XbaI	5′ggggtacccctgtctgaatatattcgggta3′	5′gctctagagcctaggcattggatatatgaacgct3′
TDP-43 (the C-terminus: amino acid residues 252–414; C)	p3XFLAG-CMV7.1	KpnI, XbaI	5′ggggtaccccaaggaatcagcgttcatatatcc3′	5′gctctagagcctacattccccagccagaag3′
TDP-43 (the N-terminus: amino acid residues 3–98; N)	p3XFLAG-CMV7.1	KpnI, XbaI	5′ggggtacccctgtctgaatatattcgggta3′	5′gctctagagcctatcttttcactttcactgctga3′
TDP-43 (the RRM1 domain: amino acid residues 98–183; RRM1)	p3XFLAG-CMV7.1	KpnI, XbaI	5′ggggtaccccgagcagtccagaaaacatcc3′	5′gctctagagcctagctttgcttagaatttg3′
TDP-43 (the RRM2 domain: amino acid residues 184–258; RRM2)	p3XFLAG-CMV7.1	KpnI, XbaI	5′ggggtaccccgccaagatgagcctttgaga3′	5′gctctagagcctaggatatatgaacgctga3′
TDP-43 (the N-terminus plus the RRM1 domain: amino acid residues 3–183; NRRM1)	p3XFLAG-CMV7.1	KpnI, XbaI	5′ggggtacccctgtctgaatatattcgggta3′	5′gctctagagcctagctttgcttagaatttg3′
TDP-43 (the RRM2 domain plus the C-terminus: amino acid residues 184–414; RRM2C)	p3XFLAG-CMV7.1	KpnI, XbaI	5′ggggtaccccgccaagatgagcctttgaga3′	5′gctctagagcctacattccccagccagaag3′
TDP-43 (the full-length monomer: amino acid residues 1–414; MM)	pFN21A-CMV Flexi	SgfI, PmeI	5′cgaagcgatcgccatgtctgaatatattcgggtaa3′	5′tgtcgtttaaaccattccccagccagaagact3′
TDP-43 (the full-length tandem dimer: amino acid residues 1–414 ×2; DM)	pFN21A-CMV Flexi	SgfI, KpnI	5′cgaagcgatcgccatgtctgaatatattcgggtaa3′	5′cggggtaccccgcattccccagccagaagactt3′
		KpnI, PmeI	5′cggggtaccccgtctgaatatattcgggtaacc3′	5′tgtcgtttaaaccattccccagccagaagact3′
TDP-43 (the full-length: amino acid residues 2–414; FL)	pCMV-Myc	XhoI, NotI	5′ccgctcgagcggtgtctgaatatattcgggta3′	5′atagtttagcggccgcattcttatctacattccccagccagaaga3′
GFP	p3XFLAG-CMV7.1	EcoRI, KpnI	5′cggaattccgccagcaaaggagaagaacttt3′	5′ggggtacccctttatttgtagagctcatcca3′
GFP	pFN21A-CMV Flexi	SgfI, PmeI	5′taaagcgatcgccatggccagcaaaggagaaga3′	5′cgaggtttaaacttttgtagagctcatccatgcca3′
CSNK1A1	pEF6/V5/His-TOPO	Not necessary	5′gggatggcgagtagcagcggctccaag3′	5′gaaacctttcatgttactcttggt3′
UBQLN1	pCDNA4/HisMax-TOPO	Not necessary	5′gccgagagtggtgaaagcggcggt3′	5′ctatgatggctgggagcccagtaa3′

Genes	Cloning vectors	Restriction enzyme sites for cloning	Sense oligonucleotides	Antisense oligonucleotides
siRNA of TDP-43	pGeneClip Hygromycin	Not necessary	5′tctcggaatcagcgttcatatatcttcctgtcaatatatgaacgctgattccct3′	5′ctgcagggaatcagcgttcatatattgacaggaagatatatgaacgctgattcc3′
Scrambled sequence	pGeneClip Hygromycin	Not necessary	5′tctcgctaggtacctttgaaaatcttcctgtcaattttcaaaggtacctagcct3′	5′ctgcaggctaggtacctttgaaaattgacaggaagattttcaaaggtacctagc3′

See Fig. 1 for the structure of TDP-43 domains cloned in the vectors

TDP-43 TAR DNA-binding protein-43, *RRM* RNA recognition motif, *GFP* green fluorescent protein, *CSNKA1* casein kinase-1 alpha-1, *UBQLN1* ubiquilin-1

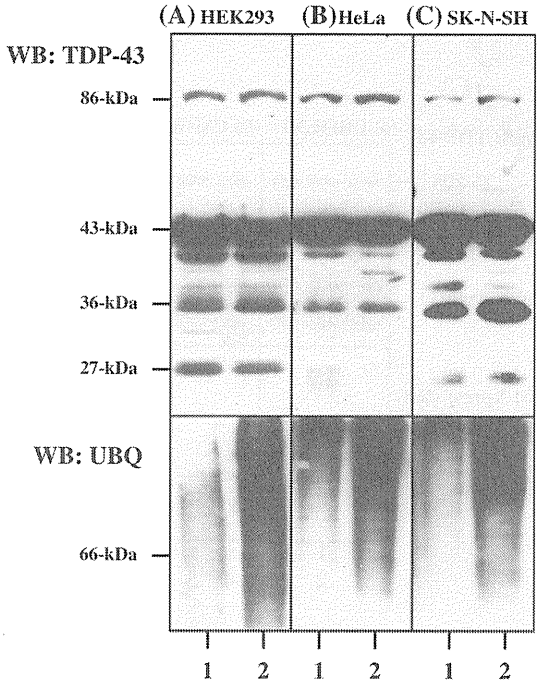

Fig. 2 The constitutive expression of an 86-kDa TDP-43-immunoreactive protein in human cell lines in culture. The detergent-soluble protein extract of HEK293, HeLa, and SK-N-SH cells exposed for 24 h to the vehicle (dimethylsulfoxide) (*lane 1*) or 1-μM MG-132 (*lane 2*) was processed for Western blot with anti-TDP43 antibody (*upper panels*) or with anti-ubiquitin antibody (*lower panels*). A small but discernible amount of the 86-kDa TDP-43-immunoreactive band is expressed in all the cells examined

cells (Fig. 3C, upper panel a, lane 3; upper panel b, lane 6). Furthermore, either a 48-h exposure of the cells to 10-nM okadaic acid, an inhibitor of protein phosphatases 1 and 2A, or a 48-h treatment with 20-μM hydrogen peroxide, an oxidative stress inducer did not alter the levels of expression of the 86-kDa protein (not shown). The use of different extraction buffers, either the M-PER protein extraction buffer or the RIPA buffer for protein extraction or the inclusion of 20-mM dithiothreitol (DTT) or an increased amount of 2-mercaptoethanol (2-ME) that reduces a typical disulfide bond in the sample-loading buffer did not affect the levels of expression of the 86-kDa protein, suggesting that the intermolecular interaction is fairly a detergent-resistant (not shown).

Next, we conducted immunoprecipitation analysis. After Flag-tagged FL TDP-43 or Flag-tagged GFP was expressed in HEK293, HeLa, and SK-N-SH cells, the protein extract was processed for immunoprecipitation with anti-Flag affinity gel. Then, the precipitates were eluted and processed for Western blot with anti-TDP-43 antibody (10782-2-AP). The proteins binding to Flag-tagged TDP-43 always included the endogenous FL TDP-43 protein in addition to several truncated species (Fig. 4A, upper panels a–c, lane 1). We identified multimeric forms of Flag-tagged TDP-43 proteins, when the immunoprecipitates were overloaded on the gel (Fig. 4B, lanes 1 and 2). In contrast, the precipitates of Flag-tagged GFP-binding proteins were completely devoid of the endogenous TDP-43 protein (Fig. 4A, upper panels a–c, lane 2). Furthermore, reciprocal immunoprecipitation analysis verified that Flag-tagged TPD-43 interacts with Myc-tagged TDP-43, excluding non-specific binding of TDP-43 to immunoglobulins (Fig. 4C, upper and lower panels, lanes 1–3). These results indicate that a substantial part of endogenous TDP-43 protein interacts with the exogenous Flag-tagged TDP-43 but not with the exogenous Flag-tagged GFP, suggesting that TDP-43 intrinsically forms the dimer, and TDP-43 forms a specific molecular interaction with TDP-43. Taken all these results together, we concluded that the 86-kDa protein represents a dimer of TDP-43.

By fractionation analysis of total cellular proteins of HEK293, the 86-kDa protein was highly enriched in the cytosolic fraction but absent in the nuclear fraction, while the 43-kDa FL endogenous TDP-43 protein was distributed in all the compartments, including cytosol, membrane, nuclear, and cytoskeletal fractions (Fig. 5, panel a, lanes 1–5).

Involvement of N-Terminal Half in Intermolecular Interaction of TDP-43 Proteins

To identify the domains involved in the intermolecular interaction of TDP43 proteins, a panel of Flag-tagged truncated proteins (Fig. 1), including the C-terminal fragment spanning amino acid residues 252–414 (C), the N-terminal fragment spanning amino acid residues 3–98 (N), the RRM1 domain spanning amino acid residues 98–183 (RRM1), the RRM2 domain spanning amino acid residues 184–258 (RRM2), the N-terminal domain plus RRM1 spanning amino acid residues 3–183 (NRRM1), the C-terminal domain plus RRM2 spanning amino acid residues 184–414 (RRM2C), and the C-terminal domain-cleaved protein spanning amino acid residues 3–260 (delC) were individually expressed in HEK293 cells. Then, the protein extract was processed for immunoprecipitation with anti-Flag affinity gel, followed by Western blot with anti-TDP-43 antibody (10782-2-AP). The anti-TDP-43 antibody (10782-2-AP) reacted with FL TDP-43, delC, N, NRRM1, RRM2, and RRM2C, but not with RRM1 or C (Fig. 6, lanes 1, 3, 5, 9, 11, and 15). These results indicate that the 10782-2-AP antibody recognizes at least two separate epitopes located in N and RRM2 in the N-terminal half of TDP-43. After immunoprecipitation, the endogenous FL TDP-43 protein was detected exclusively in the precipitates of Flag-tagged FL TDP-43, delC, and NRRM1 fragments (Fig. 6, lanes 1, 3, and 9). These results suggest that the continuous N-terminal half domain spanning amino acid

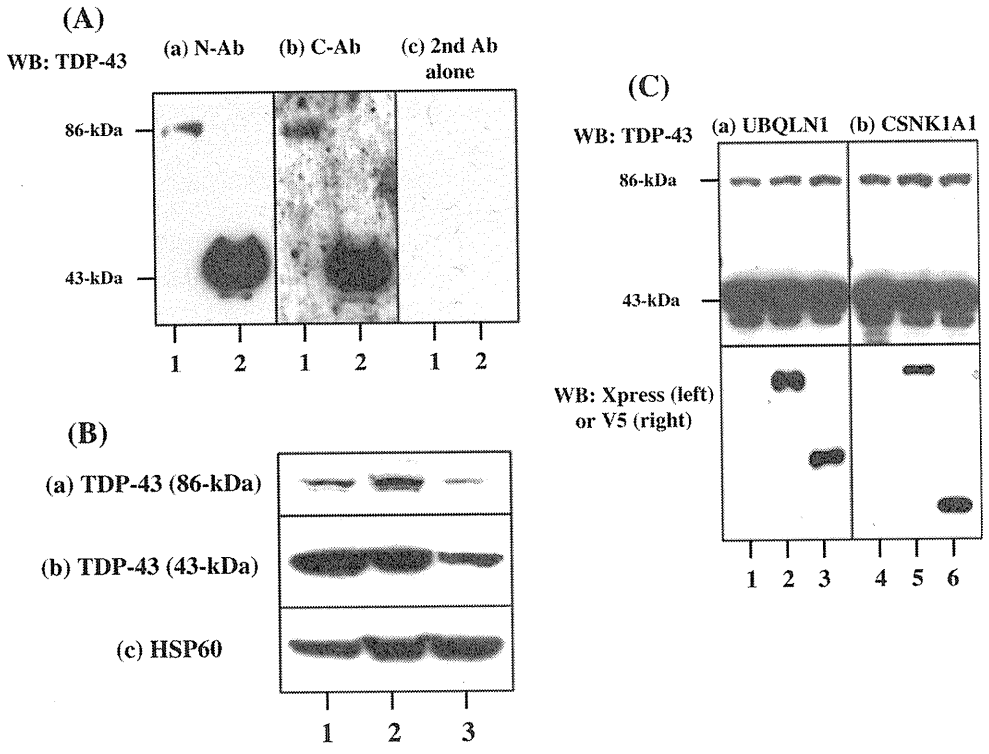

Fig. 3 The characterization of the 86-kDa protein. **A** The immunolabeling of the protein with N- or C-terminal-specific anti-TDP-43 antibodies. Both 86- and 43-kDa proteins were extracted from the corresponding SDS-PAGE gel bands, concentrated, and processed for Western blot with the N-terminal-specific anti-TDP-43 antibody (*panel a*), the C-terminal-specific anti-TDP-43 antibody (*panel b*), or the secondary antibody alone (*panel c*). The lanes (*1* and *2*) represent the 86- and the 43-kDa protein, respectively. **B** The effects of transient expression of TDP-43 siRNA. SK-N-SH cells were transfected with the siRNA expression vector targeted to TDP-43 or a scrambled sequence listed in Table 1. 96 h after transfection, the protein extract was processed for Western blot with anti-TDP-43 antibody (*panels a* and *b*) or anti-HSP60 antibody, an internal control for protein loading (*panel c*). The lanes (*1–3*) represent non-transfected cells, the cells transfected with the vector of a scrambled sequence, and the cells transfected with the vector of TDP-43 siRNA, respectively. **C** The effects of expression of ubiqulin-1 (UBQLN1) and casein kinase-1 alpha-1 (CSNK1A1). HEK293 cells were untransfected (*lanes 1* and *4*) or transfected with the expression vectors of Xpress-tagged LacZ (*lane 2*), Xpress-tagged UBQLN1 (*lane 3*), V5-tagged LacZ (*lane 5*), or V5-tagged CSNK1A1 (*lane 6*). The detergent-soluble protein extract was processed for Western blot with anti-TDP-43 antibody (*upper panels*), anti-Xpress antibody (*the left lower panel*), or anti-V5 antibody (*the right lower panel*)

residues 3–183, possibly by constructing a conformationally ordered interacting domain, but neither N nor RRM1 alone, is sufficient for the intermolecular interaction of TDP-43, while the C-terminal domain is dispensable for this.

TDP-43 Dimer Acts as a Seed for Promoting Aggregation of TDP-43 Proteins

To investigate a role of the TDP-43 dimer in TDP-43 protein aggregation, Halo-tagged TDP-43 FL monomer, tandem dimer, or GFP was expressed in HEK293 cells. Then, the blot was labeled with anti-TDP43 antibody (10782-2-AP), anti-Halo tag antibody, anti-PARP antibody, anti-ubiquitin antibody, or anti-HSP60 antibody. The expression of the TDP-43 tandem dimer but neither the monomer nor GFP greatly enhanced an accumulation of TDP-43-immunoreactive proteins with higher molecular mass ranging from 70- to 200-kDa (Fig. 7A, panel a, lane 5), while the levels of expression of Halo-tagged proteins were identical among GFP, the monomer, and the dimer (Fig. 7A, panel b, lanes 3–5). These results suggest that TDP-43 dimer by acting as a seed promotes protein aggregation that involves various endogenous species of TDP-43, including N-terminally cleaved fragments. Unexpectedly, untransfected and untreated HEK293 cells expressed constitutively both uncleaved (116-kDa) and cleaved (85-kDa) forms of PARP without morphological features of apoptosis (Fig. 7A, panel c, lanes 1–5). The expression of TDP-43 tandem dimer did not alter the levels of the cleaved PARP (Fig. 7A, panel c, lane 5) or did not elevate substantially the levels of ubiquitinated proteins, compared with the cells with expression of GFP or the monomer (Fig. 7A, panel d, lanes 3–5). In contrast, a 24-h treatment with MG-132 enhanced an accumulation of ubiquitinated proteins (Fig. 7A, panel d, lane 2). Importantly, the numbers of the cells presenting with nuclear

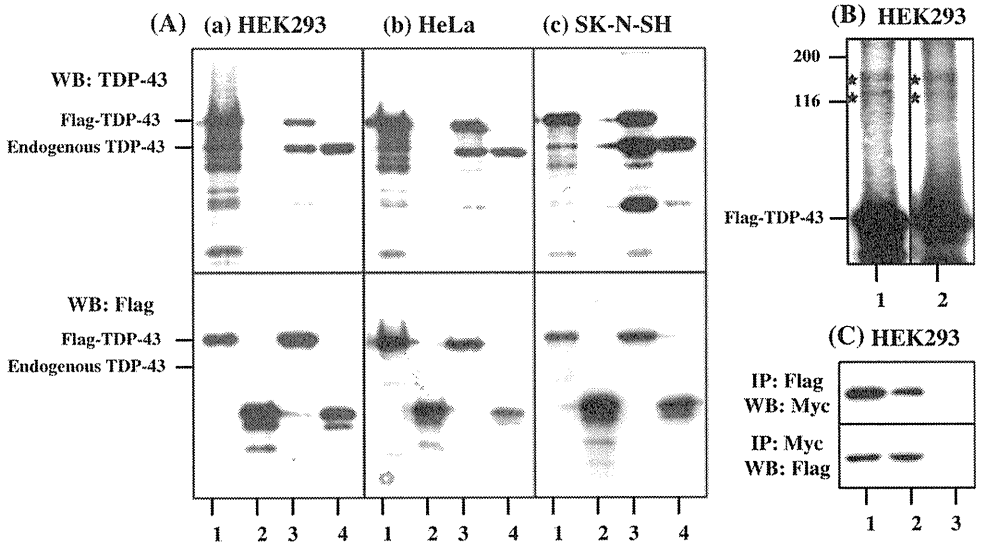

Fig. 4 Immunoprecipitation analysis of Flag-tagged TDP-43-binding proteins. A Coimmunoprecipitation with Flag-tagged proteins. Flag-tagged FL TDP-43 (*lanes 1* and *3*) or GFP (*lanes 2* and *4*) was expressed in HEK293 (*panel a*), HeLa (*panel b*), and SK-N-SH (*panel c*) cells. The detergent-soluble protein extract was processed for immunoprecipitation (IP) with anti-Flag M2 affinity gel, followed by Western blot (WB) with anti-TDP-43 antibody (*upper panels*) or anti-Flag M2 antibody (*lower panels*). The lanes (*1–4*) represent (*1* and *2*) the immunoprecipitates and (*3* and *4*) the corresponding input controls. B Flag-tagged TDP-43 constitutes multimeric forms. Flag-tagged FL TDP-43 was expressed in HEK293 cells, and then processed for IP with anti-Flag M2 affinity gel, followed by WB with anti-TDP-43 antibody or anti-Flag M2 antibody. Immunoprecipitates were overloaded on a 10% SDS–PAGE gel. The lanes (*1*, *2*) represent anti-TDP-43 antibody and anti-Flag M2 antibody, respectively. Multimeric forms are indicated by *stars*. C Reciprocal coimmunoprecipitation analysis. Flag-tagged FL TDP-43 and Myc-tagged FL TDP-43 were coexpressed in HEK293. IP followed by WB was performed using the antibody against Myc (*upper panel*) or Flag (*lower panel*), reciprocally. The lanes (*1–3*) represent input control, IP with anti-Flag M2 or anti-Myc antibody, and IP with normal mouse or rabbit IgG, respectively

accumulation of Halo tag immunoreactivity was significantly smaller in the tandem dimer-expressing HEK293 cells than those expressing the monomer ($P = 0.00008$, two-tailed Student's t test) (Fig. 7B, panels a–d and Fig. 7C).

Identification of TDP-43 Dimer in Human Brain Tissues

Finally, we conducted Western blot analysis of the detergent-soluble protein extract of human brain tissues with anti-TDP43 antibody (10782-2-AP). The expression of the 86-kDa TDP-43 dimer, along with the 43-kDa FL TDP-43 monomer and several cleaved fragments, was identified at varying levels in both the cerebrum (CBR) and the cerebellum (CBL) of the patients with PD, ALS, MS, schizophrenia, or depression (Fig. 8, panel a, lanes 1–15). Although the brain tissues derived from ALS patients constantly expressed higher levels of the TDP-43 dimer, we could not obtain the definite conclusion because of the limitation of the samples examined.

Discussion

By Western blot analysis, we identified the expression of the 86-kDa TDP-43-immunoreactive protein in HEK293, HeLa, and SK-N-SH cells in culture. We considered this protein as a dimer of TDP-43 for the following reasons. First, the molecular weight of the protein corresponds exactly to that of the dimer. Second, two different anti-TDP-43 antibodies that recognize distinct antigenic epitopes located in the N- or the C-terminal domain equally labeled the 86-kDa protein, excluding the possibility of immunological cross reactivity on a non-TDP-43 protein. Third, the levels of expression of the 86-kDa protein were greatly reduced by treatment with TDP-43 siRNA, suggesting that it is composed of TDP-43. Fourth, by immunoprecipitation analysis, we verified the interaction between the endogenous FL TDP-43 and the exogenous Flag-tagged TDP-43. We excluded non-specific binding of TDP-43 to immunoglobulins. We identified the N-terminal half spanning amino acid residues 3–183 as an intermolecular interacting domain. Finally, the 86-kDa protein was identified in human brain tissues of various neurological diseases, arguing against the possibility of an in vitro artificial byproduct. Nevertheless, we could not completely exclude the possibility that the 86-kDa protein represents a complex of TDP-43 with an unidentified 43-kDa protein. It is of particular interest that SDS-resistant dimers of DJ-1, whose loss of function causes PD, are accumulated in PD and AD brains (Choi et al. 2006).

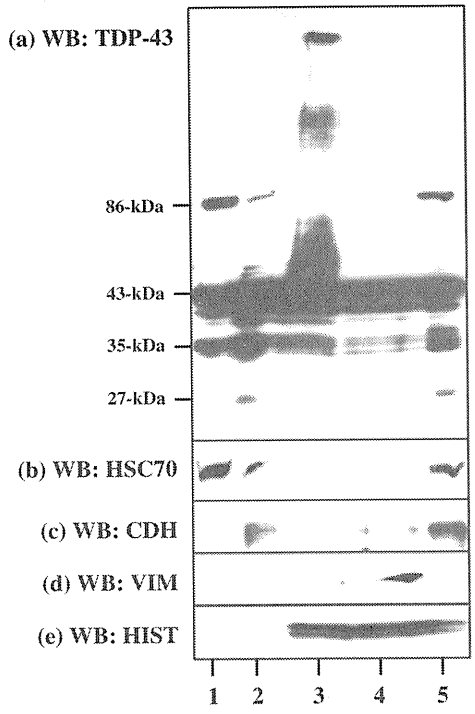

Fig. 5 Fractionation analysis of cellular proteins of HEK293. The cellular proteins of HEK293 separated into cytosol (*lane 1*), membrane (*lane 2*), nuclear (*lane 3*), and cytoskeletal (*lane 4*) fractions were processed for Western blot with anti-TDP-43 antibody (*panel a*), anti-HSC70 antibody (*panel b*), anti-pan-cadherin antibody (*panel c*), anti-vimentin antibody (*panel d*), and anti-histone H1 antibody (*panel e*). The lane (*5*) represents the unfractionated input control

Supporting our observations, a recent crystal structural study has clarified the self-assembling capacity of TDP-43 (Kuo et al. 2009). Another study showed that Flag-tagged FL TDP-43 protein binds to GFP-tagged C-terminally deleted products of TDP-43, suggesting a role of the N-terminal domain in the intermolecular interaction (Zhang et al. 2009). In contrast, a different study disclosed that the wild-type human TDP-43 protein has an intrinsically aggregation-prone propensity that requires the C-terminal domain (Johnson et al. 2009). Furthermore, DsRed-tagged FL TDP-43 is colocalized in cytoplasmic inclusions with GFP-tagged C-terminal fragments (Nonaka et al. 2009a). These observations suggest the possibility that the dimer formation of TDP-43 requires the N-terminal half, while afterward the aggregate formation involves the C-terminal domain as well.

In contrast to the normal nuclear location of TDP-43 under physiological conditions, the pathogenic TDP-43 is often redistributed in the neuronal and glial cytoplasm and dystrophic neuritis by forming insoluble aggregates (Arai et al. 2006; Neumann et al. 2006). Importantly, we found that the 86-kDa TDP-43 dimer was enriched in the cytosolic fraction in HEK293 cells. When the 86-kDa tandemly connected dimer of TDP-43 was overexpressed in HEK293, it also showed a trend for being distributed outside the nucleus, and promoted an accumulation of high-molecular-mass TDP-43-immunoreactive proteins. These observations propose the working hypothesis that a very small amount of TDP-43 dimer expressed constitutively in normal cells under physiological conditions might serve as a starting seed that triggers aggregation of posttranslationally modified TDP-43 species under pathological conditions of TDP-43 proteinopathy.

A previous study showed that TDP-43 continuously shuttles between the nucleus and the cytoplasm in a transcription-dependent manner (Ayala et al. 2008). Because TDP-43 plays a key role in shuttling of mRNA species in response to the neuronal injury (Moisse et al. 2009), even a trivial perturbation affecting the nucleocytoplasmic

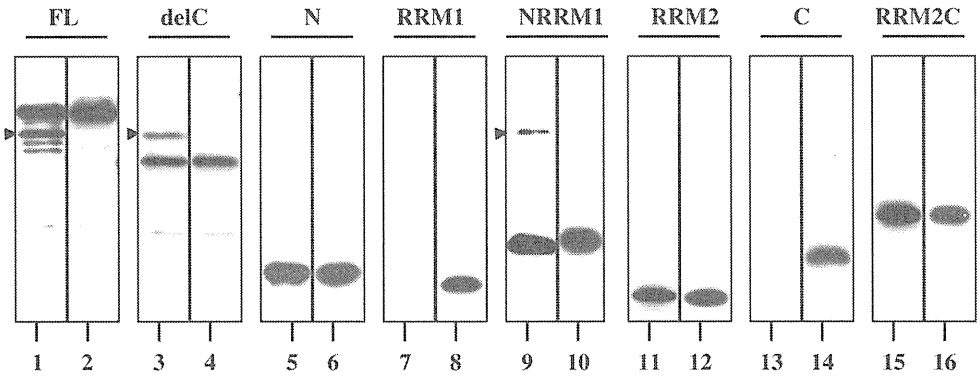

Fig. 6 The domains involved in the intermolecular interaction of TDP-43 proteins. Flag-tagged FL TDP-43 (*lanes 1* and *2*) and a panel of truncated proteins (see the details in Fig. 1), including delC (*lanes 3* and *4*), N (*lanes 5* and *6*), RRM1 (*lanes 7* and *8*), NRRM1 (*lanes 9* and *10*), RRM2 (*lanes 11* and *12*), C (*lanes 13* and *14*), and RRM2C (*lanes 15* and *16*) were individually expressed in HEK293 cells. The protein extract was processed for IP with anti-Flag affinity gel, followed by Western blot with anti-TDP-43 antibody (*lanes 1, 3, 5, 7, 9, 11, 13,* and *15*) or anti-Flag M2 antibody (*lanes 2, 4, 6, 8, 10, 12, 14,* and *16*). The position (43-kDa) of the immunoprecipitated endogenous FL TDP-43 is indicated by *arrow heads*

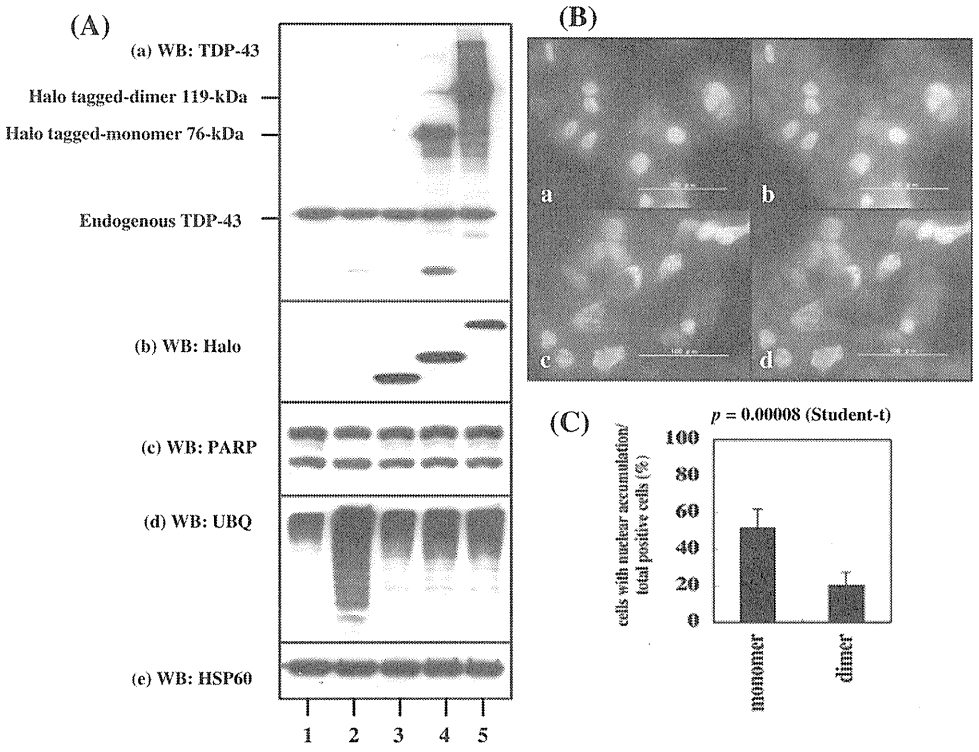

Fig. 7 TDP-43 dimer serves as a seed for promoting aggregation of TDP-43 proteins. A The expression of TDP-43 tandem dimer promotes an accumulation of high-molecular-mass TDP-43-immunoreactive proteins. The vectors of Halo-tagged GFP (*lane 3*), TDP-43 FL monomer (*lane 4*), or FL tandem dimer (*lane 5*) were transfected or untransfected (*lanes 1* and *2*) in HEK293 cells with (*lane 2*) or without (*lanes 1, 3–5*) a 24-h treatment of 1-μM MG-132. The protein extract was processed for Western blot with anti-TDP43 antibody (*panel a*), anti-Halo tag antibody (*panel b*), anti-PARP antibody (*panel c*), anti-ubiquitin antibody (*panel d*), or anti-HSP60 antibody, an internal control for protein loading (*panel e*). B Cell imaging analysis. HEK293 cells expressing Halo-tagged TDP-43 monomer (*panels a* and *b*) or tandem dimer (*panels c* and *d*) were processed for labeling with Oregon Green (*panels a* and *c*) merged with nuclear labeling with DAPI (*panels b* and *d*). C The counting of the number of the cells with nuclear accumulation of Halo-tagged proteins. The average of cell counts of six random fields under the magnification of ×400 is shown with standard deviations

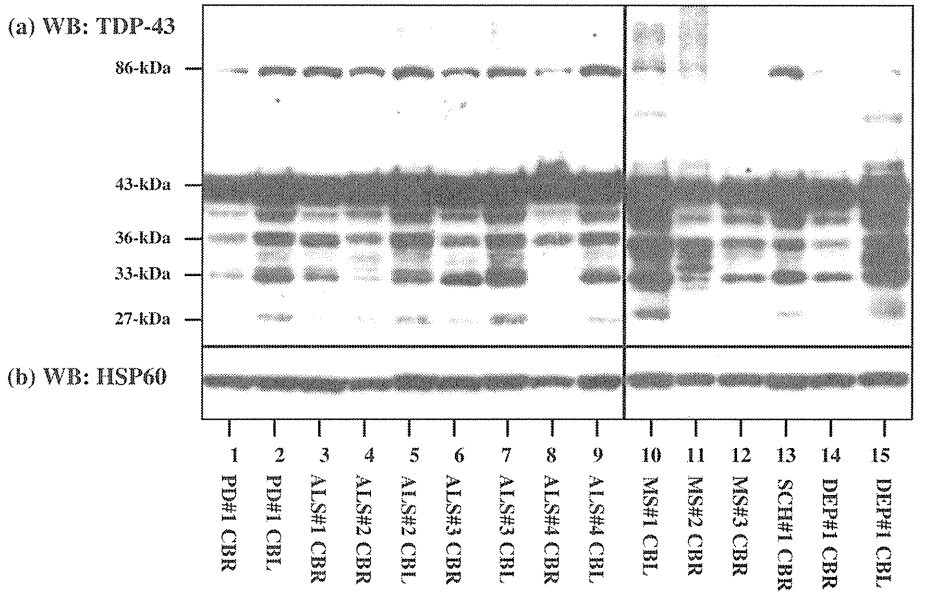

Fig. 8 The constitutive expression of TDP-43 dimer in human brain tissues. The detergent-soluble protein extract of human brain tissues of the cerebrum (*CBR*) (*lanes 1, 3, 4, 6, 8, 11–14*) and the cerebellum (*CBL*) (*lanes 2, 5, 7, 9, 10, 15*), derived from PD#1 (*lanes 1* and *2*), ALS#1 (*lane 3*), ALS#2 (*lanes 4* and *5*), ALS#3 (*lanes 6* and *7*), ALS#4 (*lanes 8* and *9*), MS#1 (*lane 10*), MS#2 (*lane 11*), MS#3 (*lane 12*), SCH#1 (*lane 13*), and DEP#1 (*lanes 14* and *15*) was processed for Western blot with anti-TDP43 antibody (*upper panels*) or anti-HSP60 antibody, an internal control for protein loading (*lower panels*)

transport of TDP-43 could disturb neuronal function by deregulating gene expression. TDP-43 accumulates in the cytoplasm following inhibition of RNA polymerase II by treatment with actinomycin D (Ayala et al. 2008). The C-terminal domain is the most important part for maintenance of solubility and cellular localization of TDP-43, while disruption of the RRM1 domain increases TDP-43 binding to the chromatin and nuclear matrix (Ayala et al. 2008). The TDP-43 mutant protein defective in the nuclear localization signal (NLS) forms cytoplasmic aggregates, while the mutant defective in the nuclear export signal (NES) constitutes nuclear aggregates (Winton et al. 2008). Inhibition of proteasome function by MG-132 enhances the aggregate formation in the NLS-defective mutant (Nonaka et al. 2009b). The overexpression of TDP-43 C-terminal fragment is sufficient to generate hyperphosphorylated and ubiquitinated cytoplasmic aggregates that could alter the exon splicing pattern (Zhang et al. 2009). Although overexpression of the wild-type human TDP-43 protein is toxic to yeast and rat cells (Johnson et al. 2008; Tatom et al. 2009), overexpression of the tandem dimer of TDP-43 did not cause acute cytotoxicity in HEK293 cells in this study.

In this study, the levels of expression of TDP-43 dimer were unaltered in HEK293 cells by treatment with MG-132 or overexpression of ubiqulin-1 (UBQLN1). The ubiqulin family proteins, composed of an N-terminus ubiquitin-like (UBL) domain and a C-terminal ubiquitin-associated (UBA) domain separated by a central Sti1-like repeat, physically interact with both proteasomes and ubiquitin ligases (Ford and Monteiro 2006). UBQLN1, capable of forming a dimer via the central region, promotes the formation of cytoplasmic aggregates of TDP-43, and regulates the proteasome and autophagosome targeting of TDP-43 aggregates (Kim et al. 2008). Polyubiquitinated TDP-43 interacts with the UBA domain of UBQLN1 (Kim et al. 2008). We found that following the expression of the tandem TDP-43 dimer, accumulated high-molecular-mass TDP-43-immunoreactive proteins are unlikely to be ubiquitinated. The 86-kDa TDP-43 dimer constitutively expressed in cultured human cells might not interact with UBQLN1, because it is unlikely to be modified by polyubiquitination.

The present observations suggest that the 86-kDa TDP-43-immunoreactive protein represents a very small amount of dimerized TDP-43 expressed constitutively in normal cells under physiological conditions. We suppose that this dimerized TDP-43 might serve as a starting seed that triggers aggregation of TDP-43 under pathological conditions of TDP-43 proteinopathy. This hypothesis warrants further immunohistochemical and neurochemical investigations, including the establishment of TDP-43-dimer-specific antibodies.

Acknowledgments Human brain tissues were provided by Research Resource Network (RRN), Japan. This work was supported by a research grant to J-IS from the High-Tech Research Center Project, the Ministry of Education, Culture, Sports, Science and Technology (MEXT), Japan (S0801043) and a grant from Research on Intractable Diseases, the Ministry of Health, Labour and Welfare of Japan.

References

Arai T, Hasegawa M, Akiyama H, Ikeda K, Nonaka T, Mori H, Mann D, Tsuchiya K, Yoshida M, Hashizume Y, Oda T (2006) TDP-43 is a component of ubiquitin-positive tau-negative inclusions in frontotemporal lobar degeneration and amyotrophic lateral sclerosis. Biochem Biophys Res Commun 351:602–611

Ayala YM, Pantano S, D'Ambrogio A, Buratti E, Brindisi A, Marchetti C, Romano M, Baralle FE (2005) Human, Drosophila, and *C. elegans* TDP43: nucleic acid binding properties and splicing regulatory function. J Mol Biol 348:575–588

Ayala YM, Zago P, D'Ambrogio A, Xu YF, Petrucelli L, Buratti E, Baralle FE (2008) Structural determinants of the cellular localization and shuttling of TDP-43. J Cell Sci 121:3778–3785

Buratti E, Baralle FE (2008) Multiple roles of TDP-43 in gene expression, splicing regulation, and human disease. Front Biosci 13:867–878

Buratti E, Brindisi A, Giombi M, Tisminetzky S, Ayala YM, Baralle FE (2005) TDP-43 binds heterogeneous nuclear ribonucleoprotein A/B through its C-terminal tail: an important region for the inhibition of cystic fibrosis transmembrane conductance regulator exon 9 splicing. J Biol Chem 280:37572–37584

Choi J, Sullards MC, Olzmann JA, Rees HD, Weintraub ST, Bostwick DE, Gearing M, Levey AI, Chin LS, Li L (2006) Oxidative damage of DJ-1 is linked to sporadic Parkinson and Alzheimer diseases. J Biol Chem 281:10816–10824

Ford DL, Monteiro MJ (2006) Dimerization of ubiquilin is dependent upon the central region of the protein: evidence that the monomer, but not the dimer, is involved in binding presenilins. Biochem J 399:397–404

Geser F, Martinez-Lage M, Kwong LK, Lee VM, Trojanowski JQ (2009) Amyotrophic lateral sclerosis, frontotemporal dementia and beyond: the TDP-43 diseases. J Neurol 256:1205–1214

Hasegawa M, Arai T, Nonaka T, Kametani F, Yoshida M, Hashizume Y, Beach TG, Buratti E, Baralle F, Morita M, Nakano I, Oda T, Tsuchiya K, Akiyama H (2008) Phosphorylated TDP-43 in frontotemporal lobar degeneration and amyotrophic lateral sclerosis. Ann Neurol 64:60–70

Johnson BS, McCaffery JM, Lindquist S, Gitler AD (2008) A yeast TDP-43 proteinopathy model: exploring the molecular determinants of TDP-43 aggregation and cellular toxicity. Proc Natl Acad Sci USA 105:6439–6444

Johnson BS, Snead D, Lee JJ, McCaffery JM, Shorter J, Gitler AD (2009) TDP-43 is intrinsically aggregation-prone and ALS-linked mutations accelerate aggregation and increase toxicity. J Biol Chem 284:20329–20339

Kabashi E, Valdmanis PN, Dion P, Spiegelman D, McConkey BJ, Vande Velde C, Bouchard JP, Lacomblez L, Pochigaeva K, Salachas F, Pradat PF, Camu W, Meininger V, Dupre N, Rouleau GA (2008) TARDBP mutations in individuals with sporadic and familial amyotrophic lateral sclerosis. Nat Genet 40:572–574

Kametani F, Nonaka T, Suzuki T, Arai T, Dohmae N, Akiyama H, Hasegawa M (2009) Identification of casein kinase-1 phosphorylation sites on TDP-43. Biochem Biophys Res Commun 382:405–409

Kim SH, Shi Y, Hanson KA, Williams LM, Sakasai R, Bowler MJ, Tibbetts RS (2008) Potentiation of ALS-associated TDP-43 aggregation by the proteasome-targeting factor, Ubiquilin 1. J Biol Chem 284:8083–8092

Kuo PH, Doudeva LG, Wang YT, Shen CK, Yuan HS (2009) Structural insights into TDP-43 in nucleic-acid binding and domain interactions. Nucleic Acids Res 37:1799–1808

Moisse K, Volkening K, Leystra-Lantz C, Welch I, Hill T, Strong MJ (2009) Divergent patterns of cytosolic TDP-43 and neuronal progranulin expression following axotomy: implications for TDP-43 in the physiological response to neuronal injury. Brain Res 1249:202–211

Neumann M, Sampathu DM, Kwong LK, Truax AC, Micsenyi MC, Chou TT, Bruce J, Schuck T, Grossman M, Clark CM, McCluskey LF, Miller BL, Masliah E, Mackenzie IR, Feldman H, Feiden W, Kretzschmar HA, Trojanowski JQ, Lee VM (2006) Ubiquitinated TDP-43 in frontotemporal lobar degeneration and amyotrophic lateral sclerosis. Science 314:130–133

Neumann M, Kwong LK, Lee EB, Kremmer E, Flatley A, Xu Y, Forman MS, Troost D, Kretzschmar HA, Trojanowski JQ, Lee VM (2009) Phosphorylation of S409/410 of TDP-43 is a consistent feature in all sporadic and familial forms of TDP-43 proteinopathies. Acta Neuropathol 117:137–149

Nonaka T, Kametani F, Arai T, Akiyama H, Hasegawa M (2009a) Truncation and pathogenic mutations facilitate the formation of intracellular aggregates of TDP-43. Hum Mol Genet 18: 3353–3364

Nonaka T, Arai T, Buratti E, Baralle FE, Akiyama H, Hasegawa M (2009b) Phosphorylated and ubiquitinated TDP-43 pathological inclusions in ALS and FTLD-U are recapitulated in SH-SY5Y cells. FEBS Lett 583:394–400

Ou SH, Wu F, Harrich D, García-Martínez LF, Gaynor RB (1995) Cloning and characterization of a novel cellular protein, TDP-43, that binds to human immunodeficiency virus type 1 TAR DNA sequence motifs. J Virol 69:3584–3596

Satoh J, Obayashi S, Misawa T, Sumiyoshi K, Oosumi K, Tabunoki H (2009) Protein microarray analysis identifies human cellular prion protein interactors. Neuropathol Appl Neurobiol 35:16–35

Tatom JB, Wang DB, Dayton RD, Skalli O, Hutton ML, Dickson DW, Klein RL (2009) Mimicking aspects of frontotemporal lobar degeneration and Lou Gehrig's disease in rats via TDP-43 overexpression. Mol Ther 17:607–613

Wang IF, Wu LS, Shen CK (2008) TDP-43: an emerging new player in neurodegenerative diseases. Trends Mol Med 14:479–485

Winton MJ, Igaz LM, Wong MM, Kwong LK, Trojanowski JQ, Lee VM (2008) Disturbance of nuclear and cytoplasmic TAR DNA-binding protein (TDP-43) induces disease-like redistribution, sequestration, and aggregate formation. J Biol Chem 283: 13302–13309

Zhang YJ, Xu YF, Dickey CA, Buratti E, Baralle F, Bailey R, Pickering-Brown S, Dickson D, Petrucelli L (2007) Progranulin mediates caspase-dependent cleavage of TAR DNA binding protein-43. J Neurosci 27:10530–10534

Zhang YJ, Xu YF, Cook C, Gendron TF, Roettges P, Link CD, Lin WL, Tong J, Castanedes-Casey M, Ash P, Gass J, Rangachari V, Buratti E, Baralle F, Golde TE, Dickson DW, Petrucelli L (2009) Aberrant cleavage of TDP-43 enhances aggregation and cellular toxicity. Proc Natl Acad Sci USA 106:7607–7612

Neuropathology and Applied Neurobiology (2010), **36**, 320–330 doi: 10.1111/j.1365-2990.2010.01076.x

Aberrant microRNA expression in the brains of neurodegenerative diseases: miR-29a decreased in Alzheimer disease brains targets neurone navigator 3

M. Shioya*, S. Obayashi*, H. Tabunoki*, K. Arima†, Y. Saito‡, T. Ishida§ and J. Satoh*

**Department of Bioinformatics and Molecular Neuropathology, Meiji Pharmaceutical University, †Department of Psychiatry, National Center Hospital, NCNP, ‡Department of Laboratory Medicine, National Center Hospital, NCNP, Tokyo, and §Department of Pathology and Laboratory Medicine, Kohnodai Hospital, International Medical Center, Chiba, Japan*

M. Shioya, S. Obayashi, H. Tabunoki, K. Arima, Y. Saito, T. Ishida and J. Satoh (2010) *Neuropathology and Applied Neurobiology* 36, 320–330

Aberrant microRNA expression in the brains of neurodegenerative diseases: miR-29a decreased in Alzheimer disease brains targets neurone navigator 3

Aims: MicroRNAs (miRNAs) are small non-coding RNAs that regulate translational repression of target mRNAs. Accumulating evidence indicates that various miRNAs, expressed in a spatially and temporally controlled that manner in the brain plays a key role in neuronal development. However, at present, the pathological implication of aberrant miRNA expression in neurodegenerative events remains largely unknown. To identify miRNAs closely associated with neurodegeneration, we performed miRNA expression profiling of brain tissues of various neurodegenerative diseases. **Methods:** We initially studied the frontal cortex derived from three amyotrophic lateral sclerosis patients by using a microarray of 723 human miRNAs. This was followed by enlargement of study population with quantitative RT-PCR analysis ($n = 21$). **Results:** By microarray analysis, we identified up-regulation of miR-29a, miR-29b and miR-338-3p in amyotrophic lateral sclerosis brains, but due to a great interindividual variation, we could not validate these results by quantitative RT-PCR. However, we found significant down-regulation of miR-29a in Alzheimer disease (AD) brains. The database search on TargetScan, PicTar and miRBase Target identified neurone navigator 3 (NAV3), a regulator of axon guidance, as a principal target of miR-29a, and actually NAV3 mRNA levels were elevated in AD brains. MiR-29a-mediated down-regulation of NAV3 was verified by the luciferase reporter assay. By immunohistochemistry, NAV3 expression was most evidently enhanced in degenerating pyramidal neurones in the cerebral cortex of AD. **Conclusions:** These observations suggest the hypothesis that underexpression of miR-29a affects neurodegenerative processes by enhancing neuronal NAV3 expression in AD brains.

Keywords: Alzheimer disease, bioinformatics, microarray, miR-29a, neurone navigator 3, real-time RT-PCR

Introduction

MicroRNAs (miRNAs) constitute a class of endogenous small non-coding RNAs conserved through the evolution [1]. miRNAs mediate post-transcriptional regulation of protein-coding genes by binding to the 3′ untranslated region (3′UTR) of target mRNAs, leading to translational inhibition or mRNA degradation, depending on the degree of sequence complementarity. The primary miRNAs are transcribed from the intra- and inter-genetic regions of the genome by RNA polymerase II, followed by processing by the RNase III enzyme Drosha into pre-miRNAs. After

Correspondence: Jun-ichi Satoh, Department of Bioinformatics and Molecular Neuropathology, Meiji Pharmaceutical University, 2-522-1 Noshio, Kiyose, Tokyo 204-8588, Japan. Tel: +81 42 4958678; Fax: +81 42 4958678; E-mail: satoj@my-pharm.ac.jp

nuclear export, they are cleaved by the RNase III enzyme Dicer into mature miRNAs consisting of approximately 22 nucleotides. Finally, a single-stranded miRNA is loaded on to the RNA-induced silencing complex, where the seed sequence located at positions 2–8 from the 5′ end of the miRNA plays a pivotal role in binding to the target mRNA. The miRNAs in a whole cell regulate approximately 30% of all protein-coding genes [2]. A single miRNA is capable of reducing the production of hundreds of proteins [3]. Thus, by targeting multiple transcripts and affecting expression of numerous proteins, miRNAs play a key role in cellular development, differentiation, proliferation, apoptosis and metabolism.

Increasing evidence indicated that various miRNAs, expressed in a spatially and temporally controlled manner in the brain, are involved in neuronal development, differentiation and synaptic plasticity [4]. miR-134 localized to the synaptodendritic compartment of hippocampal neurones regulates synaptic plasticity by inhibiting translation of Lim-domain-containing protein kinase 1 [5]. miR-30a-5p, a miRNA enriched in layer III pyramidal neurones in the human prefrontal cortex, decreases brain-derived neurotrophic factor protein levels [6]. Because a single miRNA has a great impact on the expression of numerous downstream mRNA targets, deregulation of miRNA function in the brain affects diverse cellular signalling pathways essential for neuronal survival and protection against neurodegeneration [7].

The transcription factor Pitx3 indispensable for differentiation of dopaminergic neurones transcribes miR-133b, which in turn suppresses Pitx3 expression [8]. The levels of expression of miR-133b are substantially reduced in dopaminergic neurones in Parkinson disease (PD) brains [8]. The expression of miR-107 that inhibits the production of the β-site amyloid precursor protein cleaving enzyme 1 (BACE1) is reduced in the cerebral cortex of the patients with Alzheimer disease (AD) in the earliest stage [9]. BACE1 is also a target gene for miR-29, and the expression of miR-29a/b-1 cluster is reduced, inversely correlated with BACE1 protein levels, in the anterior temporal cortex of a subgroup of AD patients [10]. The levels of miR-298 and miR-328, both of which decrease the expression of mouse BACE1 protein, are reduced in the hippocampus of aged APPSwe/PS1 transgenic mice [11]. The expression of miR-106b that targets amyloid precursor protein is decreased in the anterior temporal cortex of AD patients [12]. Up-regulation of the nuclear factor NFκB-responsive miR-146a induces down-regulation of complement factor H, an anti-inflammatory mediator in AD brains [13]. Although approximately 70% of presently identified miRNAs are expressed in the brain, physiological and pathogenetic roles of most of these remain unknown [14].

In the present study, to identify miRNAs aberrantly expressed in the brains of human neurodegenerative diseases, we initially studied miRNA expression profiles of the frontal cortex of three amyotrophic lateral sclerosis (ALS) patients on a miRNA microarray. Following enlargement of the study population, we found significant down-regulation of miR-29a in AD brains, being consistent with the previous observations [10]. We identified neurone navigator 3 (NAV3) as a principal target of miR-29a by bioinformatics database search and luciferase reporter assay. NAV3 expression was most evidently enhanced in degenerating pyramidal neurones in the cerebral cortex of AD. These results suggest that the interaction between miR-29a and NAV3 might play a role in neurodegenerative processes of AD.

Materials and methods

Human brain tissues

All the brain tissues of the frontal cortex were obtained from Research Resource Network, Japan. Written informed consent was obtained at autopsy form all the cases examined. The Ethics Committee of both National Center of Neurology and Psychiatry and International Medical Center of Japan approved the present study. The present study includes seven AD patients composed of four men and three women with the mean age of 69.1 ± 9.2 years, and 14 non-AD patients composed of eight men and six women with the mean age of 73.1 ± 10.1 years. The latter include four patients with PD, six patients with ALS and four subjects who died of non-neurological causes. The neuropsychiatric disease patients were clinically diagnosed as AD, PD or ALS by board-certified neurologists and psychiatrists, and the clinical diagnosis was verified by comprehensive examination of autopsied brains by three certified neuropathologists (KA, YS, TI). All AD cases were satisfied with the Consortium to Establish a Registry for Alzheimer's Disease criteria for diagnosis of definite AD [15], and were categorized into the stage C or B of amyloid deposition and the stage VI or IV of neurofibrillary degeneration, following the Braak staging system [16]. The *post mortem* interval of

the cases ranges from 1.1 to 14 h with the average interval of 5.5 ± 4.1 h before freezing the brain tissues for storage at −80°C. Although a recent study showed limited stability of specific brain-enriched miRNAs [17], we found that the quality of RNA of frozen brain tissues with *post mortem* interval longer than 10 h is still sufficient for microarray analysis (data not shown). The characteristics of the study population are summarized in Table S1 online.

MiRNA expression profiling

Total RNA enriched in miRNA was isolated from frozen brain tissues by using mirVana miRNA isolation kit (Ambion, Austin, TX, USA). We initially studied RNA samples isolated from the frontal cortex of three ALS patients. They were individually processed for miRNA expression profiling on a human miRNA microarray version 2 (Agilent Technologies, Palo Alto, CA, USA). The array includes 723 human miRNAs based on the miRBase release 10.1 (http://microrna.sanger.ac.uk). The human frontal cortex total RNA of a 79-year-old Caucasian man who died of bladder cancer (AM6810, Ambion) was utilized as a universal reference. The quality of RNA was validated by identification of 18S rRNA and 28S rRNA peaks on Agilent 2100 Bioanalyzer with a RNA 6000 nano kit (Agilent Technologies). Microarray analysis was performed according to the manufacturer's instruction. In brief, 100 nanogram of total RNA was dephosphorylated by calf intestine alkaline phosphatase (Takara Bio, Shiga, Japan). Three prime end of dephosphorylated RNA was labelled with Cyanine 3-cytidine bisphosphate by T4 RNA ligase. The microarray was hybridized with labelled RNA at 55°C for 20 h, washed, and processed for scanning on an Agilent microarray scanner. The signal intensity was quantified by using Feature Extraction Software version 9.9.3.1 (Agilent Technologies).

Quantitative real-time RT-PCR

To quantify miRNA expression levels, TaqMan microRNA assay-based quantitative RT-PCR (qRT-PCR) was performed on the 7500 Fast Real-Time PCR system (Applied Biosystems, Foster City, CA, USA), following the Delta-Delta Ct method. RNU6B was utilized for an endogenous reference to standardize miRNA expression levels. All the data were calibrated by the universal reference data.

DNase-treated total RNA was processed for cDNA synthesis using oligo$(dT)_{20}$ primers and SuperScript II reverse transcriptase (Invitrogen, Carlsbad, CA, USA). To quantify mRNA expression levels, cDNA was amplified by qRT-PCR on the LightCycler ST300 (Roche Diagnostics, Tokyo, Japan) using SYBR Green I and the NAV3 primer sets consisting of 5′tgacccagagttgtggtctccaag3′ and 5′gtccagtttg gctatcccatgtgc3′. The expression levels of target genes were standardized against those of the glyceraldehyde-3-phosphate dehydrogenase gene detected in identical cDNA samples. All the assays were performed in triplicate.

MiRNA target prediction

The target mRNAs that have the potential binding sites for individual miRNAs were identified by searching them on public databases endowed with prediction algorithms, such as TargetScan (http://targetscan.org), PicTar (http://pictar.mdc-berlin.de) and miRBase Target (http://www.mirbase.org) [18].

Reporter assay

The precursor of hsa-miR-29a (GeneBank Accession No. AF017104) was amplified by PCR with PfuTurbo DNA polymerase (Stratagene, La Jolla, CA, USA) and a set of sense and antisense primers composed of 5′cgggatc ccgctggatttagtaagatttgggccct3′ and 5′cccaagcttgggaacg gtcaccaatacatttcctc3′. Then, it was cloned in the expression vector pBApo-CMV-Neo (Takara Bio) at the BamHI/HindIII cloning site. The 3′UTR sequence of the human NAV3 gene spanning the nucleotide position 379727-380353 that surrounds a conserved miR-29a target sequence 5′aggaacatttcctatggtgctg3′ (GenBank Accession No. NC_000012) was amplified by PCR with a set of sense and antisense primers composed of 5′ctaggcgatcgcaca aatccaagaggccagtcctc3′ and 5′ctaggtttaaacctctttcactta gaactggatgg3′. Then, it was cloned in the dual luciferase reporter vector psiCHECK2 (Promega, Madison, WI, USA) at the SgfI/PmeI cloning site. In this construct, a 6-bp deletion was introduced in the miR-29a seed sequence 5′atggtgctg3′ of the NAV3 3′UTR by using QuikChange II XL site-directed mutagenesis kit (Stratagene). The psiCHECK2 vector contains the *Renilla* luciferase gene to monitor expression changes of the target gene in addition to the firefly luciferase gene controlled by a HSV-TK promoter to normalize the transfection efficacy. At 24 h after cotransfection of the miR-29a expression vector and the

luciferase reporter vector in HEK293 cells, cell lysate was processed for dual luciferase assay on a 20/20 Luminometer (Promega). All the assays were performed in triplicate.

Western blot analysis

To prepare total protein extract, frozen brain tissues were homogenized in RIPA lysis buffer composed of a cocktail of protease inhibitors (Sigma, St. Louis, MO, USA), followed by centrifugation at 13 400 g for 5 min at room temperature (RT). The supernatant was collected for separation on a 12% SDS-PAGE gel. The protein concentration was determined by a Bradford assay kit (Bio-Rad, Hercules, CA, USA). After gel electrophoresis, the protein was transferred onto nitrocellulose membranes, which were immunolabelled at RT overnight with rabbit anti-NAV3 antibody (ab69868; Abcam Japan, Tokyo, Japan). We validated the specificity of the ab69868 antibody by Western blot of a truncated NAV3 protein spanning amino acid residues 1366–1688 (data not shown). The membranes were incubated at RT for 30 min with horseradish peroxidase-conjugated anti-rabbit or goat IgG (Santa Cruz Biotechnology). The specific reaction was visualized by using a chemiluminescent substrate (Pierce, Rockford, IL, USA). After the antibodies were stripped by incubating the membranes at 50°C for 30 min in stripping buffer composed of 62.5 mM Tris-HCl, pH 6.7, 2% SDS and 100 mM 2-mercaptoethanol, they were processed for relabeling with rabbit antibody against 14-3-3 protein (sc-629; Santa Cruz Biotechnology), an internal control for protein loading.

Immunohistochemistry

After deparaffination, tissue sections were heated in 10 mM citrate sodium buffer, pH 6.0 by autoclave at 125°C for 30 s in a temperature-controlled pressure chamber (Dako, Tokyo, Japan). They were exposed to 3% hydrogen peroxide-containing methanol at RT for 15 min to block the endogenous peroxidase activity. The tissue sections were then incubated with phosphate-buffered saline containing 10% normal goat serum at RT for 15 min to block non-specific staining. The tissue sections were incubated in a moist chamber at 4°C overnight with rabbit anti-NAV3 antibody (ab69868). After washing with phosphate-buffered saline, they were labelled at RT for 30 min with a horseradish peroxidase-conjugated secondary antibody (Nichirei, Tokyo, Japan), followed by incubation with a colorizing solution containing diaminobenzidine tetrahydrochloride. For double immunolabelling, after inactivating all the antibodies by autoclaving the sections in the citrate sodium buffer, the tissue sections were incubated with mouse anti-amyloid-beta (Aβ) 11–28 peptide antibody (12B2; Immuno-Biological Laboratories, Gunma, Japan) or rabbit anti-tau antibody (paired 356; AnaSpec, San Jose, CA, USA) at 4°C overnight, followed by incubation with alkaline phosphatase-conjugated secondary antibody (Nichirei), and colorized with New Fuchsin substrate. All the sections were exposed to a counterstain with haematoxylin. For negative controls, the step of incubation with primary antibodies was omitted.

Results

The expression of miR-29a is reduced in the frontal cortex of AD

To identify miRNAs aberrantly expressed in the brains of human neurodegenerative diseases, we initially conducted miRNA expression profiling of frozen brain tissues derived from the frontal cortex of three ALS patients on a microarray. All microarray data are shown in Table S2 online. They were filtered through the following stringent criteria, i.e. the detection of all signals above the threshold, the reference signal value exceeding 100, and the fold change expressed as the signal of ALS divided by the signal of the universal reference greater than 5. After filtration, we identified only three miRNAs, including miR-29a, miR-29b and miR-338-3p, as a group of miRNAs whose expression is substantially up-regulated in all three ALS brains (Table 1). Importantly, rodent cortical neurones express both miR-29a and miR-338-3p [19]. Because miR-29a and miR-29b are located on the identical MIRN29B/MIRN29A gene cluster on chromosome 7q32.3, their putative biological functions are similar [10]. Thereafter, we focused our attention solely on miR-29a and miR-338-3p.

Next, we increased the number of the cases to validate microarray data by qRT-PCR. They include four non-neurological controls (NC), six patients with ALS, seven with AD and four with PD. All qPCR data of individual subjects are shown in Table S3 online. Although we observed a trend for up-regulation in the levels of miR-29a expression in ALS *vs.* NC, the difference did not reach

Table 1. Three microRNAs up-regulated in ALS brains identified by microarray analysis

MicroRNA name	*Accession no.*	*Mature miR sequence*	*Chromosome location*	*Genome context*	*Fold change in ALS-case 1*	*Fold change in ALS-case 2*	*Fold change in ALS-case 4*
hsa-miR-29a	MIMAT0000086	UAGCACCAUCUGAAAUCGGUUA	7q32.3	AC016831.7; intron 2	7.5	11.7	6.3
hsa-miR-29b	MIMAT0000100	UAGCACCAUUUGAAAUCAGUGUU	7q32.3	AC016831.7; intron 2	26.5	41.3	24.2
hsa-miR-338-3p	MIMAT0000763	UCCAGCAUCAGUGAUUUUGUUG	17q25.3	AATK; intron 6, intron 7	15.3	16.0	12.7

RNA samples isolated from frozen frontal cortex tissues of three ALS patients (cases 1, 2 and 4) and a universal reference were processed for miRNA expression profiling on a microarray. The fold change is expressed as the signal of ALS divided by the signal of the universal reference.
ALS, amyotrophic lateral sclerosis.

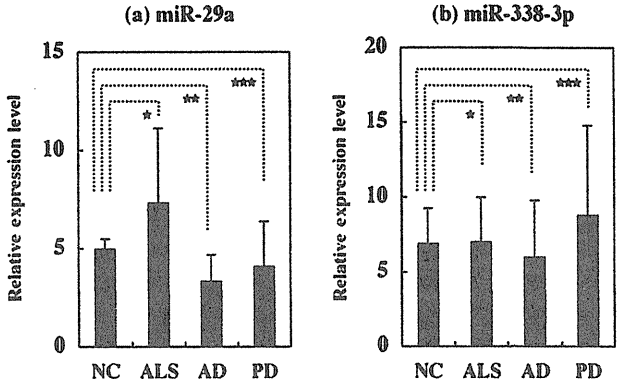

Figure 1. MiR-29a and miR-338-3p expression levels in the brains of neurodegenerative diseases. The expression of microRNA was studied in frozen frontal cortex tissues of non-neurological controls (NC) ($n = 4$), amyotrophic lateral sclerosis (ALS, $n = 6$), Parkinson disease (PD, $n = 4$) and Alzheimer disease (AD, $n = 7$) by TaqMan microRNA assay-based quantitative RT-PCR following the Delta-Delta Ct method. RNU6B was utilized for an endogenous reference to standardize microRNA expression levels. The results were expressed as relative expression levels after calibration with the universal reference data. The panels (a,b) represent (a) miR-29a and (b) miR-338-3p. The *P*-value by Student's *t*-test indicates (a) ★ 0.263, ★★ 0.041, ★★★ 0.470 and (b) ★ 0.956, ★★ 0.676, ★★★ 0.578.

the statistical significance ($P = 0.263$), due to a great interindividual variation (Figure 1a). Nevertheless, we found that miR-29a expression levels were significantly reduced in AD ($P = 0.041$), when compared with NC, while the levels of miR-29a expression were not substantially decreased in PD ($P = 0.470$) (Figure 1a). On the other hand, the levels of miR-338-3p expression were varied among the cases, and not significantly different among ALS ($P = 0.956$), AD ($P = 0.676$) and PD ($P = 0.578$), when compared with NC (Figure 1b).

Database search suggests NAV3 as one of miR-29a targets

Next, we explored putative miR-29a target genes by searching them on three distinct web-accessible miRNA target databases, including TargetScan, PicTar and miRBase Target [18], all of which did not always suggest an identical list of target genes. They identified numerous candidates, which are arranged in order of the highest probability. When top 200 most reliable miR-29a targets identified by each programme were compared, we found 11 genes shared among the three programmes (Table 2). They include fibrillin 1, NAV3, collagen, type V, alpha 3, collagen, type XI, alpha 1, collagen, type I, alpha 2,

Table 2. Predicted miR-29a target genes identified by TargetScan, PicTar and miRBase Target database search

Gene ID	*Gene symbol*	*Gene name*	*TargetScan context score*	*PicTar score*	*miRbase Target p-value*
2200	FBN1	Fibrillin 1	−0.74	8.2288	5.99E-06
89795	NAV3	Neurone navigator 3	−0.68	9.1594	1.15E-04
50509	COL5A3	Collagen, type V, alpha 3	−0.67	12.5665	1.20E-06
1301	COL11A1	Collagen, type XI, alpha 1	−0.65	10.916	5.12E-06
1278	COL1A2	Collagen, type I, alpha 2	−0.63	10.8218	2.80E-04
4678	NASP	Nuclear autoantigenic sperm protein	−0.62	9.5118	1.88E-04
4591	TRIM37	Tripartite motif-containing 37	−0.44	5.6973	2.50E-05
27315	PGAP2	Post-GPI attachment to proteins 2	−0.42	6.0952	1.28E-05
1293	COL6A3	Collagen, type VI, alpha 3	−0.4	6.9128	2.47E-07
29851	ICOS	Inducible T cell co-stimulator	−0.38	7.9789	9.64E-05
116931	MED12L	Mediator complex subunit 12-like	−0.34	9.9157	1.16E-04

MiR-29a target genes were searched on TargetScan, PicTar and miRBase Target databases. The common genes listed within top 200 by each programme are shown following the significance of TargetScan context score.

nuclear autoantigenic sperm protein, tripartite motif-containing 37, post-GPI attachment to proteins 2, collagen, type VI, alpha 3, inducible T cell co-stimulator and mediator complex subunit 12-like. Thus, the genes encoding extracellular matrix components are enriched in the list of miR-29a targets. Among them, we focused our attention on NAV3 for further investigations, because NAV3, alternatively named pore membrane and/or filament interacting like protein 1, is predominantly expressed in the nervous system [20].

MiR-29a directly down-regulates NAV3 expression

The TargetScan search indicated that the 3′UTR of the human NAV3 gene contains two separate miR-29a-binding seed sequences that are conserved through evolution. They are located in the nucleotide position 807–813 with TargetScan context score −0.24 and the position 1831–1837 with TargetScan context score −0.33. We cloned the former with the higher score in the luciferase reporter vector. Then, it was cotransfected with a miR-29a expression vector in HEK293 cells. Overexpression of miR-29a significantly suppressed the expression of the luciferase reporter containing the wild-type target sequence with a % reduction = 24.4 ($P = 0.014$; Figure 2, left panels). In contrast, miR-29a did not affect the expression of the vector containing a 6-bp deletion in the seed sequence ($P = 0.138$; Figure 2, right panels).

The levels of NAV3 mRNA but not of protein are elevated in AD brains

By qRT-PCR analysis, we found that the levels of NAV3 mRNA expression in the frontal cortex were much higher in AD patients, compared with NC subjects, PD patients and ALS patients (Figure 3). By Western blot analysis, the levels of expression of NAV3 protein, composed of two major bands of 100 kDa and 46 kDa, were varied among the cases and not elevated in AD brains, while the levels of 14-3-3 protein, an internal control for protein loading, were almost constant (Figure 4a,b, lanes 1–21). There did not exist a clear correlation between NAV3 mRNA and protein levels in each case.

Pyramidal neurones express intense NAV3 immunoreactivity in the frontal cortex of AD brains

Finally, by immunohistochemistry, we investigated the expression of NAV3 in the frontal cortex of AD, ALS or PD. In all the brains examined, large- and medium-sized pyramidal neurones in layers III and V of the cerebral cortex expressed strong NAV3 immunoreactivity located chiefly in the cytoplasm, axons and dendrites (Figure 5a–d). Notably, NAV3 immunolabelling was the most intense in neurones presenting with degenerating morphology bearing pyknotic nuclei in AD brains (Figure 5a,b,f). A population of non-pyramidal neurones also expressed much weaker NAV3 immunoreactivity, while the great majority of reactive astrocytes, microglia and

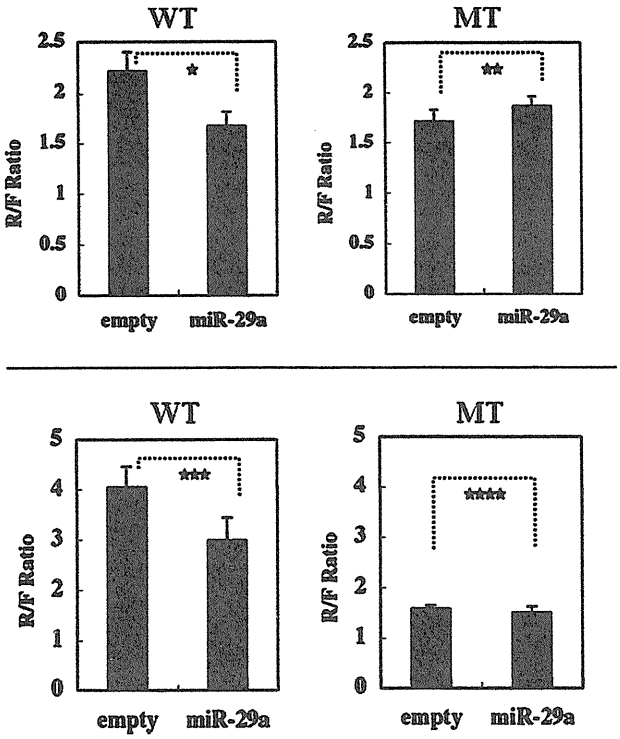

Figure 2. Dual luciferase assay of miR-29a-mediated down-regulation of neurone navigator 3 (NAV3). The precursor of hsa-miR-29a sequence was cloned in the expression vector pBApo-CMV-Neo, while the 3′ untranslated region (3′UTR) sequence of the human NAV3 was cloned in the dual luciferase reporter vector psiCHECK2 that contains the *Renilla* (R) luciferase gene to monitor expression changes of NAV3 in addition to the firefly (F) luciferase gene to normalize the transfection efficacy. A 6-bp deletion was introduced in the miR-29a seed sequence 5′ATGGTGCTG3′ of the NAV3 3′UTR. At 24 h after cotransfection of the miR-29a expression vector or the empty pBApo-CMV-Neo vector with the luciferase reporter vector in HEK293 cells, cell lysate was processed for dual luciferase assay. Two series of the experiments were performed. Each set represents the reporter vector containing (the left) the wild-type (WT) NAV3 3′UTR or (the right) the 6-bp deletion mutant (MT) NAV3 3′UTR. The R/F signal ratio is shown. The *P*-value by Student's *t*-test indicates ★ 0.014, ★★ 0.138, ★★★ 0.037 and ★★★★ 0.289.

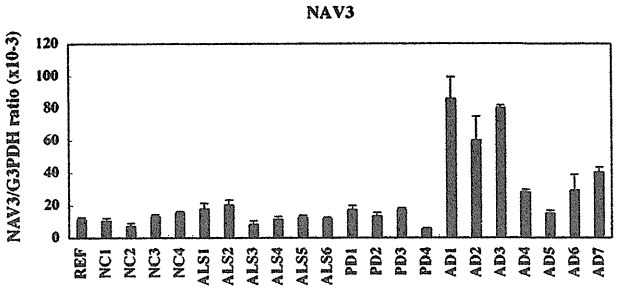

Figure 3. Neurone navigator 3 (NAV3) mRNA expression levels in the brains of neurodegenerative diseases. The expression of NAV3 mRNA was studied in frozen frontal cortex tissues of non-neurological controls (NC, $n = 4$), amyotrophic lateral sclerosis (ALS, $n = 6$), Parkinson disease (PD, $n = 4$) and Alzheimer disease (AD, $n = 7$) by quantitative RT-PCR. The levels of NAV3 mRNA are standardized against those of glyceraldehyde-3-phosphate dehydrogenase (G3PDH) mRNA detected in identical cDNA samples. REF indicates a universal reference derived from the human frontal cortex total RNA (AM6810, Ambion).

oligodendrocytes are devoid of NAV3. In AD brains, a substantial population (<20%) of pyramidal neurones containing tau-immunolabelled neurofibrillary tangles coexpressed intense NAV3 immunoreactivity (Figure 5e). In contrast, Aβ plaques did not typically express NAV3 immunoreactivity in AD brains (Figure 5f).

Discussion

To identify miRNAs aberrantly regulated in the brains of human neurodegenerative diseases, we initially studied miRNA expression profiles of frozen frontal cortex tissues of three ALS patients by using a miRNA microarray. We identified up-regulation of miR-29a, miR-29b and miR-338-3p in ALS brains. Among them, miR-338 is a biomarker candidate for neurodegeneration, because it acts as a negative regulator of neuronal differentiation by suppressing apoptosis-associated tyrosine kinase and cytochrome oxidase complex IV [21,22]. However, following enlargement of the study population by qRT-PCR, we could not verify up-regulation of miR-338-3p in ALS brains. On the other hand, we identified significant down-regulation of miR-29a in AD brains, being consistent with previous observations that miR-29 expression levels are reduced in the anterior temporal cortex of AD patients, associated with substantial elevation of BACE1 protein levels [10]. However, in the present study, the search on three distinct miRNA target databases, such as TargetScan, PicTar and miRBase Target operating on different algorithms, did not identify BACE1 within the top 200 miR-29a targets. These programmes commonly identified NAV3 as one of top-ranking miR-29a targets. We verified the miR-29a-mediated suppression of NAV3 by luciferase reporter assay.

Previous studies showed that miR-29 is involved in translational repression of a wide range of target genes. Down-regulation of miR-29 in the area surrounding the myocardial infarct core enhances fibrosis by de-repressing the expression of a battery of collagen genes [23]. miR-29a represses translation of osteonectin, the most abundant non-collagenous matrix protein in the bone [24]. In

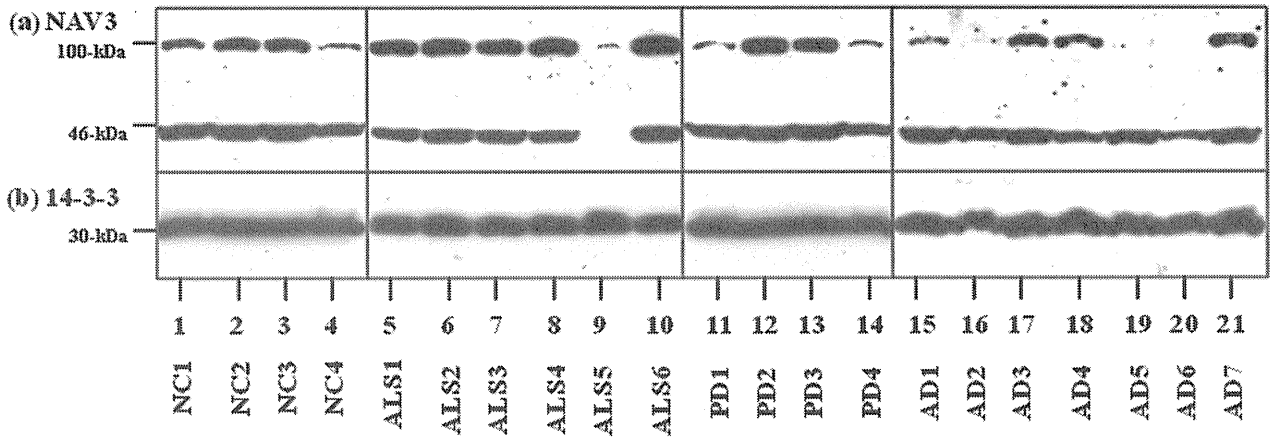

Figure 4. Neurone navigator 3 (NAV3) protein expression levels in the brains of neurodegenerative diseases. The expression of NAV3 protein was studied in frozen frontal cortex tissues of non-neurological controls (NC), amyotrophic lateral sclerosis (ALS), Parkinson disease (PD) and Alzheimer disease (AD) by Western blot. The panels (a, b) indicate (a) NAV3 protein and (b) 14-3-3 protein, an internal control for protein loading. The lanes (1–21) represent (1–4) NC, (5–10) ALS, (11–14) PD and (15–21) AD. Eighty micrograms of protein was loaded in each lane.

line with these, we identified a panel of extracellular matrix components, such as fibrillin 1, collagen, type V, alpha 3, collagen, type XI, alpha 1 and collagen, type I, alpha 2, as a group of top-ranking miR-29a target genes. The levels of expression of the miR-29 family are reduced in lung cancer, cholangiocarcinoma, chronic lymphocytic leukemia and neuroblastoma, suggesting that miR-29 acts as a proapoptotic anti-oncomir [25–27]. The oncogenic transcription factor cMyc reduces the expression of miR-29 in cancer cells by binding directly to the miR-29 promoter region [28]. By suppressing the expression of PI3 kinase p85α and CDC42, miR-29 activates p53 and induces apoptosis in HeLa cells [29]. miR-29 acts as an enhancer of myogenic differentiation and a suppressor of rhabdomyosarcoma by targeting YY1 transcription factor [30]. miR-29a promotes the epithelial-to-mesenchymal transition of breast cancer cells by suppressing the expression of tristetraprolin [31]. All of these observations suggest that miR-29a modulates cellular differentiation and survival by regulating a wide range of target mRNAs.

Neurone navigator 3 is a member of the neurone navigator protein family expressed predominantly in the central and peripheral nervous systems [20]. In adult mouse brain, NAV3 is expressed chiefly in nuclear membranes of neurones in the cerebral cortex, midbrain, cerebellum and the hippocampal formation [20]. The NAV3 protein structure is characterized by an N-terminal calponin homology domain, several coiled-coil regions, an actin-binding domain, a GTP/ATP-binding domain and an AAA-type ATPase domain [32]. Although the biological function of mammalian NAV3 protein in the brain remains totally unknown, a *Caenorhabditis elegans* gene named unc-53 highly homologous to NAV3, plays a key role in axon guidance [33]. Importantly, NAV2, a paralog of NAV3, plays a central role in neurite outgrowth and axonal elongation in human neuroblastoma cells [34]. Furthermore, the NAV3 gene is occasionally disrupted in primary cutaneous T cell lymphomas by chromosomal translocation, suggesting that NAV3 acts as a tumour suppressor gene [35].

We found that the levels of NAV3 mRNA were elevated in AD brains, although we did not find a correlation between NAV3 mRNA levels by real-time RT-PCR and protein levels by Western blot. The lack of the correlation between mRNA levels and protein abundance might be in part attributable to the differential stability and turnover of mRNA and protein via various post-transcriptional mechanisms, including the selective degradation of proteins by proteasome and autophagosome machineries [36]. Nevertheless, we found that pyramidal neurones in the cerebral cortex expressed strong NAV3 immunoreactivity in both AD and non-AD brains. Furthermore, a substantial population of cortical pyramidal neurones coexpressed NAV3 and neurofibrillary tangles in AD brains, where NAV3 immunoreactivity was the most intense in neurones with degenerating morphology bearing pyknotic nuclei. A previous study performed on mouse brains showed that NAV3 immunoreactivity is

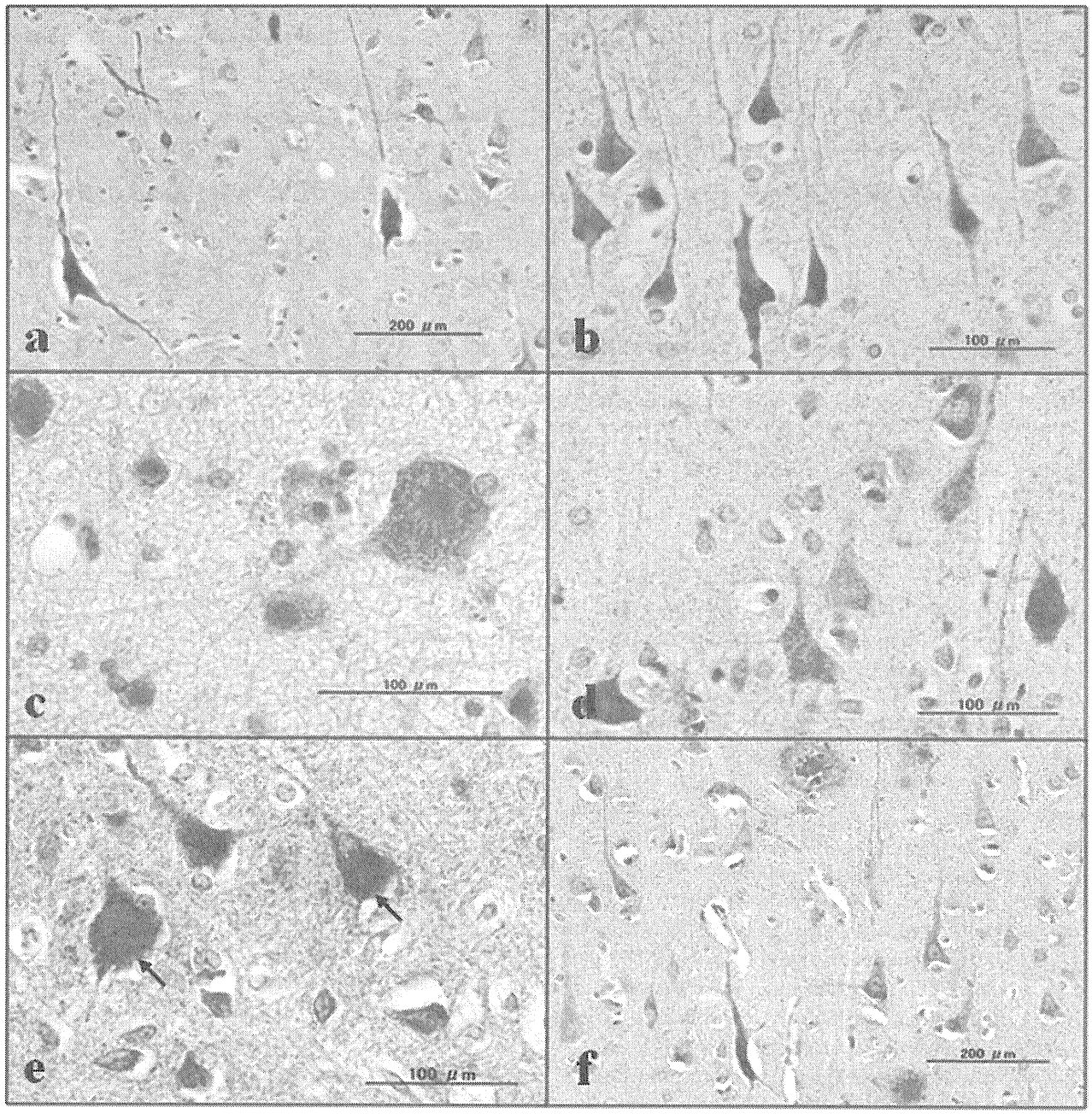

Figure 5. Neurone navigator 3 (NAV3) immunohistochemistry of the brains of neurodegenerative diseases. The expression of NAV3, paired helical filament (PHF)-tau and Aβ was studied in the frontal cortex tissue sections of Alzheimer disease (AD), amyotrophic lateral sclerosis (ALS) and Parkinson disease (PD) by immunohistochemistry. The panels (a–f) represent (a) NAV3 in AD-case 3, (b) NAV3 in AD-case 1, (c) NAV3 in ALS-case 4, (d) NAV3 in PD-case 3, (e) NAV3 (brown) and PHF-tau (red) double immunolabelling of AD-case 1 where the coexpression is indicated by arrows, and (f) NAV3 (brown) and Aβ (red) double immunolabelling of AD-case 3. In all the cases, large- and medium-sized pyramidal neurones in layers III and V express strong NAV3 immunoreactivity located in the cytoplasm, axons and dendrites. Notably, NAV3 immunoreactivity is the most intense in neurones with degenerating morphology bearing pyknotic nuclei in AD brains as shown in panels (a, b, f).

constitutively expressed at the outer nuclear membrane of neurones, and it is induced in reactive astrocytes after brain injury [20]. In contrast, we did not detect NAV3 immunoreactivity in reactive astrocytes in the brains of AD, PD and ALS. At present, it remains unknown whether enhanced expression of NAV3 in a subpopulation of cortical pyramidal neurones in AD brains reflects some pathogenetic changes or it is attributable to a compensatory mechanism against neurodegenerative events. By miRNA target database search, we found that not only miR-29, but also miR-19, miR-34 and miR-449, potentially down-regulate NAV3 expression (unpublished data), suggesting that multiple miRNAs converge on the regulation of NAV3 expression. Overall, the results of the present study could propose a possible scenario that underexpression of miR-29a affects neurodegenerative processes by up-regulating NAV3 and other miR-29a targets in AD brains. Further studies using large cohorts are required to clarify an active involvement of the miR-29a and NAV3 circuit in progression of neurodegeneration in AD.

Acknowledgements

Human brain tissues were provided by Research Resource Network, Japan. This work was supported by a research grant to J-IS from the High-Tech Research Center Project, the Ministry of Education, Culture, Sports, Science and Technology, Japan (S0801043) and a grant from Research on Intractable Diseases, the Ministry of Health, Labour and Welfare of Japan.

References

1 Kosik KS. The neuronal microRNA system. *Nat Rev Neurosci* 2006; 7: 911–20
2 Filipowicz W, Bhattacharyya SN, Sonenberg N. Mechanisms of post-transcriptional regulation by microRNAs: are the answers in sight? *Nat Rev Genet* 2008; 9: 102–14
3 Selbach M, Schwanhäusser B, Thierfelder N, Fang Z, Khanin R, Rajewsky N. Widespread changes in protein synthesis induced by microRNAs. *Nature* 2008; 455: 58–63
4 Fineberg SK, Kosik KS, Davidson BL. MicroRNAs potentiate neural development. *Neuron* 2009; 64: 303–9
5 Schratt GM, Tuebing F, Nigh EA, Kane CG, Sabatini ME, Kiebler M, Greenberg ME. A brain-specific microRNA regulates dendritic spine development. *Nature* 2006; 439: 283–9
6 Mellios N, Huang HS, Grigorenko A, Rogaev E, Akbarian S. A set of differentially expressed miRNAs, including miR-30a-5p, act as post-transcriptional inhibitors of BDNF in prefrontal cortex. *Hum Mol Genet* 2008; 17: 3030–42
7 Nelson PT, Wang WX, Rajeev BW. MicroRNAs (miRNAs) in neurodegenerative diseases. *Brain Pathol* 2008; 18: 130–8
8 Kim J, Inoue K, Ishii J, Vanti WB, Voronov SV, Murchison E, Hannon G, Abeliovich A. A MicroRNA feedback circuit in midbrain dopamine neurons. *Science* 2007; 317: 1220–4
9 Wang WX, Rajeev BW, Stromberg AJ, Ren N, Tang G, Huang Q, Rigoutsos I, Nelson PT. The expression of microRNA miR-107 decreases early in Alzheimer's disease and may accelerate disease progression through regulation of beta-site amyloid precursor protein-cleaving enzyme 1. *J Neurosci* 2008; 28: 1213–23
10 Hébert SS, Horré K, Nicolaï L, Papadopoulou AS, Mandemakers W, Silahtaroglu AN, Kauppinen S, Delacourte A, De Strooper B. Loss of microRNA cluster miR-29a/b-1 in sporadic Alzheimer's disease correlates with increased BACE1/beta-secretase expression. *Proc Natl Acad Sci USA* 2008; 105: 6415–20
11 Boissonneault V, Plante I, Rivest S, Provost P. MicroRNA-298 and microRNA-328 regulate expression of mouse β-amyloid precursor protein-converting enzyme 1. *J Biol Chem* 2009; 284: 1971–81
12 Hébert SS, Horré K, Nicolaï L, Bergmans B, Papadopoulou AS, Delacourte A, De Strooper B. MicroRNA regulation of Alzheimer's amyloid precursor protein expression. *Neurobiol Dis* 2009; 33: 422–8
13 Lukiw WJ, Zhao Y, Cui JG. An NF-κB-sensitive micro RNA-146a-mediated inflammatory circuit in Alzheimer disease and in stressed human brain cells. *J Biol Chem* 2008; 283: 31315–22
14 Kocerha J, Kauppinen S, Wahlestedt C. microRNAs in CNS Disorders. *Neuromolecular Med* 2009; 11: 162–72
15 Mirra SS, Heyman A, McKeel D, Sumi SM, Crain BJ, Brownlee LM, Vogel FS, Hughes JP, van Belle G, Berg L. The Consortium to Establish a Registry for Alzheimer's Disease (CERAD). Part II. Standardization of the neuropathologic assessment of Alzheimer's disease. *Neurology* 1991; 41: 479–86
16 Braak H, Alafuzoff I, Arzberger T, Kretzschmar H, Del Tredici K. Staging of Alzheimer disease-associated neurofibrillary pathology using paraffin sections and immunocytochemistry. *Acta Neuropathol* 2006; 112: 389–404
17 Sethi P, Lukiw WJ. Micro-RNA abundance and stability in human brain: specific alterations in Alzheimer's disease temporal lobe neocortex. *Neurosci Lett* 2009; 459: 100–4
18 Mendes ND, Freitas AT, Sagot MF. Current tools for the identification of miRNA genes and their targets. *Nucleic Acids Res* 2009; 37: 2419–33
19 Kim J, Krichevsky A, Grad Y, Hayes GD, Kosik KS, Church GM, Ruvkun G. Identification of many microRNAs that

copurify with polyribosomes in mammalian neurons. *Proc Natl Acad Sci USA* 2004; **101**: 360–5
20 Coy JF, Wiemann S, Bechmann I, Bächner D, Nitsch R, Kretz O, Christiansen H, Poustka A. Pore membrane and/or filament interacting like protein 1 (POMFIL1) is predominantly expressed in the nervous system and encodes different protein isoforms. *Gene* 2002; **290**: 73–94
21 Aschrafi A, Schwechter AD, Mameza MG, Natera-Naranjo O, Gioio AE, Kaplan BB. MicroRNA-338 regulates local cytochrome c oxidase IV mRNA levels and oxidative phosphorylation in the axons of sympathetic neurons. *J Neurosci* 2008; **28**: 12581–90
22 Barik S. An intronic microRNA silences genes that are functionally antagonistic to its host gene. *Nucleic Acids Res* 2008; **36**: 5232–41
23 van Rooij E, Sutherland LB, Thatcher JE, DiMaio JM, Naseem RH, Marshall WS, Hill JA, Olson EN. Dysregulation of microRNAs after myocardial infarction reveals a role of miR-29 in cardiac fibrosis. *Proc Natl Acad Sci USA* 2008; **105**: 13027–32
24 Kapinas K, Kessler CB, Delany AM. miR-29 suppression of osteonectin in osteoblasts: regulation during differentiation and by canonical Wnt signaling. *J Cell Biochem* 2009; **108**: 216–24
25 Fabbri M, Garzon R, Cimmino A, Liu Z, Zanesi N, Callegari E, Liu S, Alder H, Costinean S, Fernandez-Cymering C, Volinia S, Guler G, Morrison CD, Chan KK, Marcucci G, Calin GA, Huebner K, Croce CM. MicroRNA-29 family reverts aberrant methylation in lung cancer by targeting DNA methyltransferases 3A and 3B. *Proc Natl Acad Sci USA* 2007; **104**: 15805–10
26 Mott JL, Kobayashi S, Bronk SF, Gores GJ. mir-29 regulates Mcl-1 protein expression and apoptosis. *Oncogene* 2007; **26**: 6133–40
27 Xu H, Cheung IY, Guo HF, Cheung NK. MicroRNA miR-29 modulates expression of immunoinhibitory molecule B7-H3: potential implications for immune based therapy of human solid tumors. *Cancer Res* 2009; **69**: 6275–81
28 Chang TC, Yu D, Lee YS, Wentzel EA, Arking DE, West KM, Dang CV, Thomas-Tikhonenko A, Mendell JT. Widespread microRNA repression by Myc contributes to tumorigenesis. *Nat Genet* 2008; **40**: 43–50
29 Park SY, Lee JH, Ha M, Nam JW, Kim VN. miR-29 miRNAs activate p53 by targeting p85 alpha and CDC42. *Nat Struct Mol Biol* 2009; **16**: 23–9
30 Wang H, Garzon R, Sun H, Ladner KJ, Singh R, Dahlman J, Cheng A, Hall BM, Qualman SJ, Chandler DS, Croce CM, Guttridge DC. NF-kappaB-YY1-miR-29 regulatory circuitry in skeletal myogenesis and rhabdomyosarcoma. *Cancer Cell* 2008; **14**: 369–81
31 Gebeshuber CA, Zatloukal K, Martinez J. miR-29a suppresses tristetraprolin, which is a regulator of epithelial polarity and metastasis. *EMBO Rep* 2009; **10**: 400–5
32 Maes T, Barceló A, Buesa C. Neuron navigator: a human gene family with homology to *unc-53*, a cell guidance gene from *Caenorhabditis elegans*. *Genomics* 2002; **80**: 21–30
33 Hekimi S, Kershaw D. Axonal guidance defects in a *Caenorhabditis elegans* mutant reveal cell-extrinsic determinants of neuronal morphology. *J Neurosci* 1993; **13**: 4254–71
34 Muley PD, McNeill EM, Marzinke MA, Knobel KM, Barr MM, Clagett-Dame M. The atRA-responsive gene neuron navigator 2 functions in neurite outgrowth and axonal elongation. *Dev Neurobiol* 2008; **68**: 1441–53
35 Karenko L, Hahtola S, Päivinen S, Karhu R, Syrjä S, Kähkönen M, Nedoszytko B, Kytölä S, Zhou Y, Blazevic V, Pesonen M, Nevala H, Nupponen N, Sihto H, Krebs I, Poustka A, Roszkiewicz J, Saksela K, Peterson P, Visakorpi T, Ranki A. Primary cutaneous T-cell lymphomas show a deletion or translocation affecting *NAV3*, the human *UNC-53* homologue. *Cancer Res* 2005; **65**: 8101–10
36 Laloo B, Simon D, Veilla V, Lauzel D, Guyonnet-Duperat V, Moreau-Gaudry F, Sagliocco F, Grosset C. Analysis of post-transcriptional regulations by a functional, integrated, and quantitative method. *Mol Cell Proteomics* 2009; **8**: 1777–88

Supporting information

Additional Supporting Information may be found in the online version of this article:

Table S1. Characteristics of the study population.
Table S2. MicroRNA expression profiling of the frontal cortex of three ALS patients on a human miRNA microarray.
Table S3. Real-time RT-PCR analysis of miR-29a expression in the frontal cortex of human neurodegenerative diseases.

Please note: Wiley-Blackwell are not responsible for the content or functionality of any supporting materials supplied by the authors. Any queries (other than missing material) should be directed to the corresponding author for the article.

Received 18 December 2009
Accepted after revision 1 February 2010
Published online Article Accepted on 25 February 2010